High-spin states in ^{43}Sc

T. Morikawa,* M. Nakamura, and T. Sugimitsu
Department of Physics, Kyushu University, Fukuoka 812-8581, Japan

H. Kusakari
Faculty of Education, Chiba University, Chiba 263-8522, Japan

M. Oshima, Y. Toh, M. Koizumi, A. Kimura, J. Goto, and Y. Hatsukawa
Japan Atomic Energy Research Institute, Tokai-mura, Ibaraki 319-1195, Japan

M. Sugawara
Chiba Institute of Technology, Narashino, Chiba 275-0023, Japan
(Received 13 July 2004; published 29 November 2004)

High-spin states in ^{43}Sc have been investigated by using the in-beam γ-ray technique with the ^{27}Al(^{19}F,$p2n$) reaction at 50 MeV. The $J^\pi=(17/2^-)$ level at 4382 keV, the $J^\pi=(17/2^-,21/2^-)$ level at 4633 keV, and some higher-lying levels were newly identified above the $J^\pi=19/2^-$ high-spin isomer, while the quasirotational structure built on the $J^\pi=3/2^+$ state has been extended up to the terminating $J^\pi=(27/2^+)$ state. The energy levels of the observed positive-parity quasirotational band were consistent with the prediction of the shell-model calculation in $\{0d_{3/2},0f_{7/2},1p_{3/2}\}$ model space, while the $J^\pi=(17/2^-,21/2^-)$ level at 4633 keV could not be reproduced by the calculation in $\{0f1p\}$ model space.

DOI: 10.1103/PhysRevC.70.054323 PACS number(s): 21.10.Hw, 23.20.En, 23.20.Lv, 27.40.+z

I. INTRODUCTION

The ^{43}Sc nucleus has a relatively simple configuration; only one proton and two neutrons are coupled to the doubly magic ^{40}Ca core. Within this simple three-particle structure, one can expect an existence of the terminating $J^\pi=19/2^-$ state. Indeed, such a state is known to exist as the $J^\pi=19/2^-$ high-spin isomer [1,2], which can be described well with the "three−particle+^{40}Ca core." In the meantime, positive parity levels, which cannot be understood in the $\{0f_{7/2}\}^3$ model space, based upon the $J^\pi=3/2^+$ state are also known to exist [3–5]. These levels from $J^\pi=3/2^+$ to $J^\pi=15/2^+$ with regular energy spacing conform to a bandlike structure. $E2$ transitions in this bandlike structure are rather enhanced [6]. Thus, the ^{43}Sc nucleus exhibits both collective and single-particle characters in its yrast region, and provides an interesting testing ground for the study of the interplay between the single-particle and the collective degrees of freedom in the nuclei near the closed shell.

The $J^\pi=19/2^-$ isomer in ^{43}Sc is expected to possess a sizable oblate deformation of $\beta\sim-0.07$ from the measured quadrupole moment [7] and g factor [2]. Although one may not naively expect a rotational band built on the isomer, search of the low-energy transitions from the higher-lying levels to the $J^\pi=19/2^-$ isomer is very interesting from the following points of view. (a) The existence of a low-energy enhanced $E2$ transition should be evidence of a collective excitation of the isomer itself; such a collective excitation has not been observed yet. (b) Although largely deformed states in ^{43}Sc have not been discovered either, the existence of a high-spin state at a low energy relative to the isomer could be a signature of such a large deformation since the high-j orbit like $0g_{9/2}$ lowers in energy with increasing deformation.

Another interest exists in the positive-parity states. A collective bandlike structure built on the $J^\pi=3/2^+$ state has been known up to the $J^\pi=15/2^+$ state [4,5]. An interpretation as the possible $K^\pi=3/2^+$ rotational structure built on the $\{fp\}^4\{sd\}^{-1}$ configuration has been studied theoretically by Johnstone [8]. On the other hand, it is known that this bandlike structure is well described also by the ^{39}K+α cluster model [9–11]. If this bandlike structure has a predominant $\{fp\}^4\{sd\}^{-1}$ configuration, one should observe the decreasing $E2$ collectivity as the angular momentum increases and approaches the maximum value of $27/2$ in this configuration. Then, finally the $J^\pi=27/2^+$ terminating state should show up, which has not been observed until now. In the meantime, high-spin levels of $J^\pi=(25/2^+)$, $(23/2^+)$, and $(19/2^+)$ have been identified by Sheppard *et al.* [12] as being the high-spin precursors of the $J^\pi=19/2^-$ isomer. These levels have been also considered as having a predominant $\{0f_{7/2}\}^4\otimes\{0d_{3/2}\}^{-1}$ configuration. If these levels are the higher-spin members of the lower-lying bandlike structure built on the $J^\pi=3/2^+$ state, one should observe a transition connecting the $J^\pi=(19/2^+)$ and $J^\pi=15/2^+$ states with a relatively large $E2$ collectivity; no such γ-ray transition, however, has been identified so far.

Motivated by the above-mentioned interests, we carried out an experimental study of the high-spin states in ^{43}Sc. In this paper, we present the results of the experiment and discuss the high-spin structure of the ^{43}Sc nucleus.

II. EXPERIMENT AND RESULTS

The experiment was performed at the Japan Atomic Energy Research Institute (JAERI) by using the

*Electronic address: morikawa@kutl.kyushu-u.ac.jp

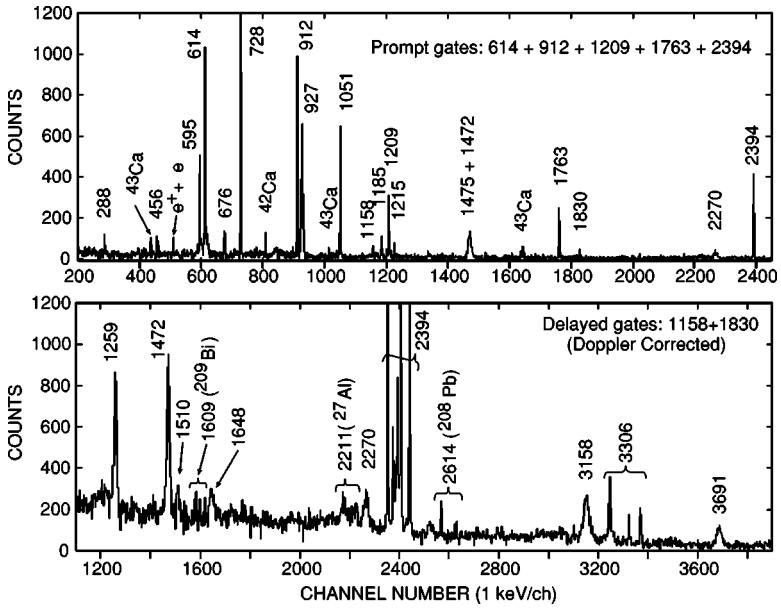

FIG. 1. Typical γ-ray energy spectra gated by the transitions in ^{43}Sc. Upper panel is the spectrum measured with the Ge detectors positioned at 90° with respect to the beam direction. Prompt gates were set on the several transitions in ^{43}Sc as indicated in the figure. A few small peaks from ^{42}Ca and ^{43}Ca contamination are also seen. Lower panel is the γ-ray spectrum which has been Doppler-corrected and summed over for all detectors. The delayed gates across the $J^{\pi}=19/2^{-}$ isomer have been set on the 1158-keV and 1830-keV transitions

^{27}Al(^{19}F,$p2n$)^{43}Sc reaction. The ^{19}F beam of 50 MeV was delivered from the JAERI Tandem Accelerator. The target was a 0.92 mg/cm^2 thick ^{27}Al foil with 10 mg/cm^2 $^{\text{nat}}$Pb backing. Prompt- and delayed-γ-γ coincidence events within the time window of ±800 ns were recorded by the γ-ray detector array GEMINI-II [13] consisting of 16 HPGe detectors with BGO anti-Compton shields. The detectors were positioned at 47° (4 Ge's), 72° (2 Ge's), 90° (2 Ge's), 105° (4 Ge's), 144° (2 Ge's), and 147° (2 Ge's) with respect to the beam direction. The Ge detectors were calibrated by using γ-ray sources of ^{152}Eu, ^{133}Ba, and ^{56}Co. The data were off-line sorted into $4k\times4k$ γ-γ correlation matrices.

Some fast γ-rays showed Doppler shift due to the large recoil velocity caused by the use of a heavy projectile. From the analysis of the Doppler shifts, mean lifetimes of the short-lived levels could be deduced, where the stopping process of recoil ^{43}Sc has been simulated by using the stopping power calculated by the program SRIM2003 [14]. In Fig. 1, a typical γ-ray spectrum measured with the Ge detectors at $\theta_{\gamma}=90°$ gated by the intense prompt transitions in ^{43}Sc is presented, together with the one Doppler-corrected and delayed-gated across the $J^{\pi}=19/2^{-}$ isomer. In the latter spectrum, one sees the fast transitions of 1259, 1510, 3158, and 3691 keV, all of which do not coincide with the transitions among the known positive-parity states. It is also seen that the stopped peaks at 1609, 2211, 2394, 2614, and 3306 keV split into separated peaks depending on the Ge positions (θ_{γ}'s) after the Doppler correction, where the 1609-, 2211-, and 2614-keV transitions were from $(n,n'\gamma)$ reactions on ^{209}Bi (BGO shield), ^{27}Al (target, target frame, and chamber), and ^{208}Pb (lead collimator of the detector), respectively. The energy of the relatively broad peak at 1648 keV fits in with the energy difference between the 1510- and 3158-keV transitions, implying that the 1510- and 1648-keV transitions are in the cascade relation and in parallel with the 3158-keV transition, which could not be clearly confirmed, however, by the γ-γ coincidence relationship due to the insufficient statistics.

The ADO ratio [15] was also analyzed in order to determine the multipolarity of the observed γ-ray transitions. The ratio was defined as $R_{\text{ADO}}=I_{\gamma}(147°)/I_{\gamma}(90°)$, where $I_{\gamma}(\theta)$ is the intensity measured by Ge detector(s) positioned at θ, with the gates being set on the coincident γ rays in any of the other Ge's. The ratio was calibrated by using the known transitions: 0.78(2) for the stretched-$E1$ transitions in ^{43}Ca and 1.34(3) for the stretched-$E2$ transitions in ^{42}Ca, respectively. In the present analysis, the ADO ratios for the known transitions in ^{43}Sc were found to be consistent with the multipolarities reported in the literatures [3–5,12].

Based on the coincidence relation, γ-ray energy sums, recoil velocities β, ADO ratios, and γ-ray intensity balance, we constructed the level scheme of ^{43}Sc as presented in Fig. 2. The γ-ray energies obtained in the present analysis involve the uncertainties of $\sim$1 keV for stopped peaks and 1–2 keV for shifted peaks due to the nonlinearity of the electronic apparatuses and the peak-fitting errors for broadened small peaks, although the energies for known transitions are in agreement with those evaluated in Refs. [16,17] within the error bars. We therefore primarily employed those evaluated values for most of the known transitions. For some transitions, however, we determined the energies from the present analysis so that the level energies and transition energies are consistent within the uncertainties.

III. DISCUSSION

A. Negative-parity states

Several transitions feeding to the negative-parity states were newly identified from the analysis of γ-ray spectra made by setting delayed and prompt gates on the transitions of 136, 1158, and 1830 keV. The 1259-keV and 1395-keV transitions were assigned as deexciting a new level of $J^{\pi}=(17/2^{-})$ at 4382 keV from the following observations. (1) Both the 1259-keV transition to the $J^{\pi}=19/2^{-}$ level and the 1395-keV transition to the $J^{\pi}=15/2^{-}$ level showed the di-

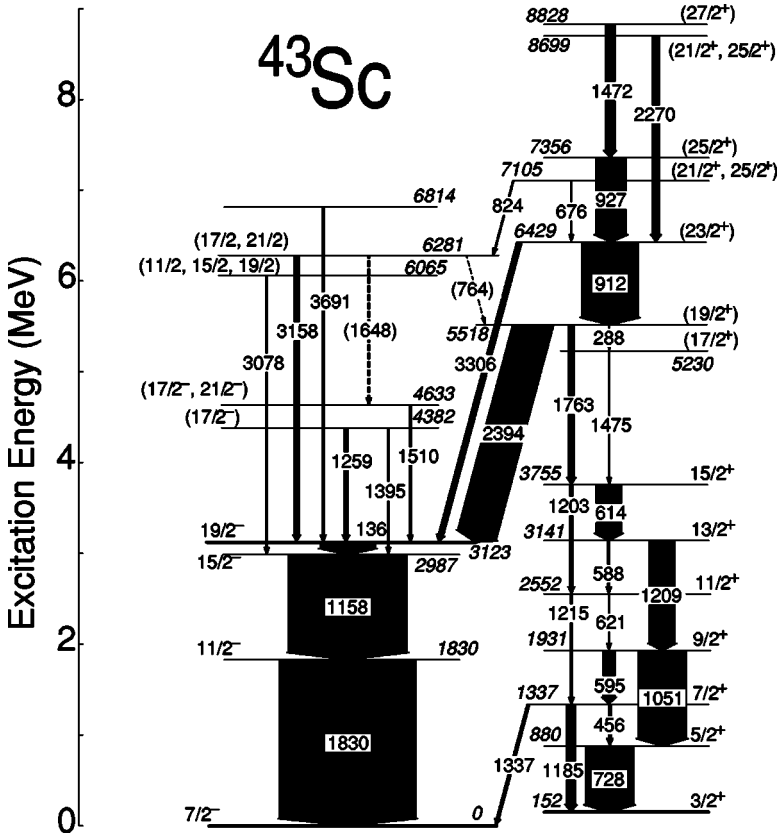

FIG. 2. Partial level scheme of ^{43}Sc proposed in the present work.

pole character. (2) The energy difference between these γ rays was found to be the same as that between the $J^\pi = 19/2^-$ and $J^\pi = 15/2^-$ levels within the experimental accuracy. (3) The Doppler shifts of both transitions gave almost the same recoil velocities (β) of 0.0282(5) for 1259 keV and 0.0283(15) for 1395 keV, respectively. The 1510-keV transition may attract one's attention because of its lowness of the energy compared with those of transitions (other than 1259 keV) feeding to the high-spin isomer. The ADO ratio of 0.86(11) for the 1510-keV transition suggests its dipole character, i.e., $M1$ or $E1$, which should be deexciting the state with $J=(17/2,21/2)$. Since no γ rays in the positive-parity yrast states were found to coincide with this 1510-keV transition, the assignment as being $E1$ may be unlikely. The 3158-keV transition also showed a stretched-dipole character. The 1648-keV transition was tentatively placed between the 6281-keV and 4633-keV levels based on the energy relation. The 3078-keV transition is either $\lambda=1, \Delta J=0$ or $\lambda=2, \Delta J=2$.

To investigate the observed levels, shell model calculations were performed by using the jj-coupled shell model code jjSMQ [18]. As to the negative-parity states, the calculation was made by taking account of the full $\{0f1p\}$ space with the realistic effective interaction FPD6 [19]. In Fig. 3, the newly identified $J^\pi=(17/2^-)$ state at 4382 keV and the $J^\pi=(17/2^-,21/2^-)$ state at 4633 keV, as well as the known yrast states of negative parity, were plotted as a function of angular momentum in comparison with results of the shell model calculations. In this figure, results of the calculation by using the surface delta interaction (SDI) [20–24] were also shown so as to give a measure of the goodness of the schematic interaction; the SDI parameters used are the same as those used in the calculation of positive-parity states discussed later. The level energy of the $J^\pi=(17/2^-)$ state as well as those of the $J^\pi=11/2^-, 15/2^-$, and $19/2^-$ states is in good agreement with the shell model calculations. In Table I, the

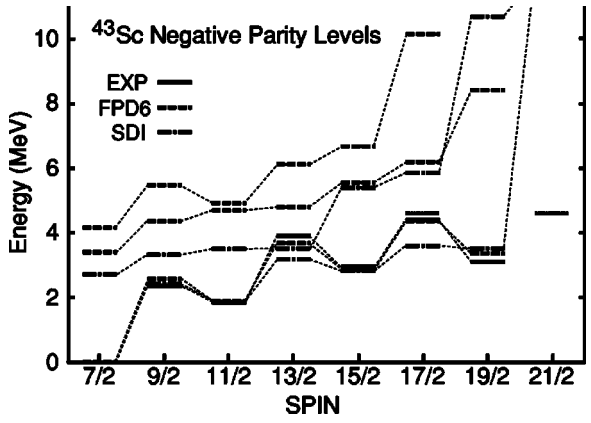

FIG. 3. A comparison of level energies between experiment and shell model calculations for negative-parity states. Solid lines are the experimental data. Dashed lines and chain lines indicate the shell model calculations by FPD6 and SDI, respectively. The FPD6 calculation was made in full $\{fp\}$ space, while the SDI calculation was done in $\pi[\{0d_{3/2}\}^k\{0f_{7/2}\}^l\{1p_{3/2}\}^{5-k-l}] \otimes \nu[\{0d_{3/2}\}^m\{0f_{7/2}\}^n\{1p_{3/2}\}^{6-m-n}]$ model space with a limitation of $0\leqslant l\leqslant 2$ and $0\leqslant n\leqslant 2$. The lowest three levels and two levels are plotted for the FPD6 and SDI calculations, respectively. A newly identified $J^\pi=(17/2^-,21/2^-)$ state at 4633 keV is indicated as dotted lines.

TABLE I. A table of electromagnetic moments and transition probabilities of ^{43}Sc. B(E2) and B(M1) values are listed in Wiesskopf unit (w.u.), while magnetic moments and Q moments are given in μ_N and $e\mathrm{fm}^2$, respectively. A common "size parameter," estimated from $\hbar\omega \sim 41A^{-1/3}$ MeV, of harmonic-oscillator wave functions was assumed. For both the FPD6 and the SDI calculations, the same effective charges and effective g factors have been used: $e_p=1.33$, $e_n=0.64$, $g_s(IS)=1.67$, $g_s(IV)=5.08$, $g_l(IS)=0.38$, and $g_l(IV)=0.33$ [19]. Level energies (E_i) and transition energies (E_γ) are given in keV.

J_i^π	J_f^π	E_i	E_γ		Exp.	FPD6	SDI[a]
$7/2^-$		0		μ	4.62(4)[b]	4.58	4.14
$7/2^-$		0		Q	−26(6)[b]	−18.4	−17.9
$11/2^-$	$7/2^-$	1830	1830	$E2$	15.4(24)[b]	4.47	4.16
$15/2^-$	$11/2^-$	2987	1158	$E2$	5.4(8)[b]	4.74	4.35
$19/2^-$		3123		Q	−19.9(14)[b]	−22.8	−22.0
$19/2^-$		3123		μ	3.122(7)[b]	3.32	2.83
$19/2^-$	$15/2^-$	3123	136	$E2$	2.93(4)[b]	2.91	3.15
$(17/2^-)$	$19/2^-$	4328	1259	$M1$	0.2(1)*[c]	1.06	1.13
$(17/2^-)$	$15/2^-$	4328	1395	$M1$	0.07(2)*[c]	0.24	0.27
$3/2^+$		152		μ	0.348(6)[b]		−0.38
$7/2^+$	$3/2^+$	1337	1185	$E2$	21(8)[b]		9.8
$9/2^+$	$7/2^+$	1931	595	$M1$	0.009(4)[b]		0.085
$9/2^+$	$7/2^+$	1931	595	$E2$	3.2(18)[b]		5.93
$9/2^+$	$5/2^+$	1931	1051	$E2$	16(5)[b]		11.7
$11/2^+$	$9/2^+$	2552	621	$M1$	0.109(17)[b]		0.20
$11/2^+$	$7/2^+$	2552	1215	$E2$	18.8[d]		14.3
$13/2^+$	$9/2^+$	3141	1209	$E2$	<45[b]		12.7
$(19/2^+)$	$15/2^+$	5518	1763	$E2$	>7.6[e]		11.2
$(23/2^+)$	$(19/2^+)$	6429	912	$E2$	5.7(6)[b]		9.9
$(25/2^+)$	$(23/2^+)$	7356	927	$M1$	0.14(3)*[c]		0.13
$(25/2^+)$	$(23/2^+)$	7356	927	$M1$	0.65(18)[b]		0.13
$(25/2^+)$	$(23/2^+)$	7356	927	$E2$	<2[f]		0.48
$(27/2^+)$	$(25/2^+)$	8828	1472	$M1$	0.10(2)[c]		0.12

[a]Calculated with condition (1) described in the text.
[b]From Ref. [16].
[c]Present work. Starred (*)= assumed to be pure $M1$.
[d]From Ref. [6].
[e]Present data + the lifetime data in Ref. [12].
[f]From Ref. [12].

measured transition probabilities and electromagnetic moments are summarized together with the results of shell model calculations. It is seen that, except for the $\mathrm{B(E2:}11/2^-\rightarrow 7/2^-\mathrm{)}$, the overall reproduction of electromagnetic properties is also pretty good for both the FPD6 and the SDI calculations. The calculated B(M1) values from the $J^\pi=(17/2^-)$ state are about a factor of 5 larger than the measured ones. This might suggest the contribution due to the higher-lying single-particle orbits which are not taken into account in the present calculations. Since the calculated B(M1) values are rather sensitive to the choice of effective g factors, we regard this discrepancy as not critical and that this $J^\pi=(17/2^-)$ state may possess a predominant $\{0f_{7/2}\}^3$ configuration.

On the other hand, the shell model calculation could not reproduce the $J^\pi=(17/2^-,21/2^-)$ state at 4633 keV; other high-spin yrare states of $\{f\,p\}^3$ structure are predicted to lie at $\geqslant$3 MeV higher than the yrast levels, which might correspond to the levels defined by the newly observed high-energy ($\geqslant$3 MeV) transitions feeding to the negative-parity levels. The absence of the corresponding $J^\pi=17/2^-$ or $21/2^-$ state in the result of the FPD6 calculation suggests that the observed state at 4633 keV has a configuration largely different from pure $\{fp\}^3$ structure. For low-lying levels in this mass region, the contribution due to the core deformation has been pointed out by several authors [7,25,26]. As suggested in Ref. [7], the core deformation may be relevant for lower-lying levels. In the present case, the discrepancy for the $\mathrm{B(E2:}11/2^-\rightarrow 7/2^-\mathrm{)}$ values between the experiment and theoretical calculations may be explained as a consequence of such a core deformation, which has not been fully taken into account due to the truncation of model space. Although such a contribution could also be present in this $J^\pi=(17/2^-,21/2^-)$ 4633 keV state since the valence $f_{7/2}$ particles being aligned to generate a large angular momentum should drive the shape of the ^{40}Ca core to oblate, the absence

of low-energy $J^\pi=8^+$ states in ^{42}Ca implies such a state in ^{43}Sc may not exist. It may also be possible that the state at 4633 keV possesses a very large deformation which could lower the energy of the higher-lying $g_{9/2}$ orbit. Further experimental investigation is highly needed for this state.

B. Positive-parity states

The positive-parity bandlike structure based on the 152 keV $J^\pi=3/2^+$ state was extended up to the $J^\pi=(27/2^+)$ state at 8828 keV. Five in-band γ-ray transitions, i.e., the 1472-, 676-, 1763-, 288-, and 1475-keV transitions, were newly identified in this band. We assigned the 1763-keV transition deexciting the $J^\pi=(19/2^+)$ state as being a stretched-$E2$ transition from its ADO ratio of 1.30(16). From the intensity ratio between the 1763-keV transition and the 2394-keV $E1$ [12] transition, and the known upper limit of the lifetime of 90 fs [12] for the $J^\pi=(19/2^+)$ state at 5518 keV, the B[E2:$(19/2^+)\rightarrow 15/2^+$] value was estimated to be $>$7.6 w.u. for the 1763-keV transition. The 1475-keV and 288-keV transitions were very weak. They are in parallel with the 1763-keV transition, but the order could not be firmly determined. We placed the 288-keV transition on top of the 1475-keV transition on the grounds that the intensity of this cascade is very small as compared to that of the 1763-keV transition. The assignment of $J^\pi=(17/2^+)$ is probable for the intermediate state at 5230 keV. The relatively intense 2270-keV transition and the 676-keV transition, both of which are feeding to the $J^\pi=(23/2^+)$ state at 6429 keV, also showed a stretched-dipole character from their ADO ratios of 0.65(12) and 0.81(10), respectively. The 824-keV transition from the 7105-keV level to the 6281-keV level gave the ADO ratio of 1.49(49), which is consistent with an interpretation as a stretched-quadrupole transition. The 1472-keV transition showed a stretched-dipole character with the ADO ratio of 0.66(7) and was placed on the $J^\pi=(25/2^+)$ state at 7356 keV from the coincidence relation.

A predominant $\{sd\}^{-1}\otimes\{fp\}^4$ structure has been suggested [8] for the lower-lying positive-parity levels of $J^\pi\leqslant 15/2^+$, while the higher-lying levels are reported [12] as having a dominant $\{0d_{3/2}\}^{-1}\otimes\{0f_{7/2}\}^4$ structure. Since these levels are connected by $E2$ transitions of a sizable collectivity, it is natural to regard these levels as being members of a bandlike sequence. By combining the estimated B[E2:$(19/2^+)\rightarrow 15/2^+$] value of $>$7.6 w.u. and those for the other $E2$ transitions summarized in Table I, a decrease of the $E2$ collectivity as increasing the angular momentum can be noticed. As to the level energies, the spacings become rather irregular above the $J^\pi=15/2^+$ state. These observations suggest a structural change with respect to the increase of angular momentum; the low-spin collective structure changes into the noncollective high-spin structure.

In order to understand the change of the structure, we carried out shell model calculations in the $\{0d_{3/2},0f_{7/2},1p_{3/2}\}$ model space. The SDI was used with the strength parameter $A_0=0.90$ and $A_1=0.56$ [27]. Single-particle energies relative to the $0d_{3/2}$ orbit were taken to be 4.9 MeV for $0f_{7/2}$ and 7.9 MeV for $1p_{3/2}$, respectively. The FPD6 interaction is not applicable in this case since it does not explicitly take into account the cross-shell excitation from the $0d_{3/2}$ orbit, which should play the dominant role for the positive-parity states in this nucleus. The SDI calculations were made for each of the following types of conditions. (1) $\pi[\{0d_{3/2}\}^k\{0f_{7/2}\}^l\{1p_{3/2}\}^{5-k-l}]\otimes\nu[\{0d_{3/2}\}^m\{0f_{7/2}\}^n\times\{1p_{3/2}\}^{6-m-n}]$ space with limitations $0\leqslant l\leqslant 2$ and $0\leqslant n\leqslant 2$. (2) Same space as (1) with $0\leqslant l\leqslant 2$ and $0\leqslant n\leqslant 4$. (3) $\pi[\{0d_{3/2}\}^k\{0f_{7/2}\}^{5-k}]\otimes\nu[\{0d_{3/2}\}^m\{0f_{7/2}\}^{6-m}]$ full space. Despite the use of a schematic interaction and the lack of $1s_{1/2}$, $1p_{1/2}$, and $0f_{5/2}$ levels, the agreement between experiment and calculation is pretty fair, as shown in Fig. 4, indicating the goodness of these model spaces. In the calculation of condition (2), eigenstates of $J^\pi\geqslant 21/2^+$ levels only could be calculated due to the limitation of the jjSMQ program. Therefore, in Fig. 4, the level energies for condition (2) are normalized to the $J^\pi=21/2^+$ state calculated with condition (1). It is seen that an inclusion of the $1p_{3/2}$ level largely improves the energy reproduction of the low-lying states, suggesting the importance of this single-particle orbit. For the highest-spin region, the calculation in full $\{0d_{3/2},0f_{7/2}\}$ space reproduces well the energy levels where the dominant $\{0d_{3/2}\}^{-1}\{0f_{7/2}\}^4$ structure is expected.

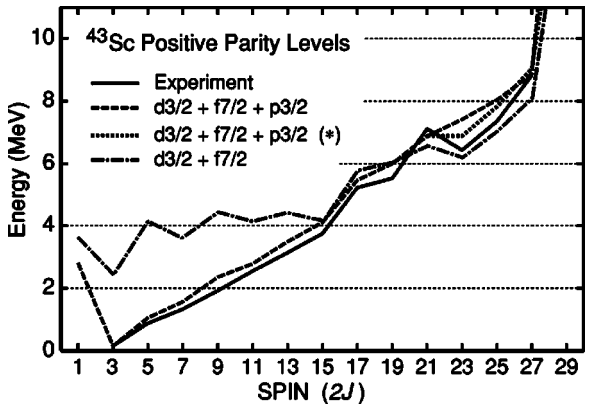

FIG. 4. A plot of level energies of positive-parity states as a function of the angular momentum. The experimental data and the SDI shell model calculations are presented. Solid line shows experimental data. The dashed line shows the positive-parity yrast levels calculated in $\pi[\{0d_{3/2}\}^k\{0f_{7/2}\}^l\{1p_{3/2}\}^{5-k-l}]\otimes\nu[\{0d_{3/2}\}^m\{0f_{7/2}\}^n\{1p_{3/2}\}^{6-m-n}]$ model space with a limitation of $0\leqslant l\leqslant 2$ and $0\leqslant n\leqslant 2$. The dotted line (*) indicates the high-spin ($J^\pi\geqslant 21/2^+$) levels calculated with a limitation of $0\leqslant l\leqslant 2$ and $0\leqslant n\leqslant 4$. The chain line is the positive-parity levels calculated in full $\{0d_{3/2},0f_{7/2}\}$ space.

As can be seen in Table I, the present calculation of condition (1) qualitatively well reproduces both the B(E2) and B(M1) values also for the positive-parity states, except those among lowest-lying levels which may be reflecting the core deformation effect. There is a discrepancy in the B(M1) values for 927-keV transition between the present work and the one reported in Ref. [12]. This might be caused by the sizable feeding from the $J^\pi=(27/2^+)$ state which has not been identified by the authors of [12], or by the neglect of a possible $E2$ contribution in the present analysis. It should be noted again that the magnetic properties obtained in the present shell model calculation are rather sensitive to the choice of the effective g factors; although the calculated

magnetic moment for the $J^\pi=3/2^+$ state in Table I has the opposite sign relative to the experimental value of $+0.348(6)\mu_N$, it was found that the use of effective g factors estimated from nucleon g factors of the $g_s^p=5.5855\ \mu_N$ and $g_s^n=-3.8256\ \mu_N$ gives a value of $\mu=+0.284\ \mu_N$, which is reasonably consistent with the experimental value.

The $J^\pi=27/2^+$ state in this model space is a kind of terminating state. The maximum angular momentum of 27/2 can be achieved by the fully stretched $\pi\{0d_{3/2}\}^{-1}\{0f_{7/2}\}^2 \otimes \nu\{0f_{7/2}\}^2$ ($\nu=5$) configuration. The states with $J^\pi \geqslant 29/2^+$ can be generated only by the $\nu \geqslant 7$ configurations, and consequently, a large energy gap between the $J^\pi=27/2^+$ and $J^\pi=29/2^+$ states is predicted. This is indeed consistent with the nonobservation of the corresponding transition in the present experiment where the γ-ray energy of only $\leqslant 4$ MeV was measured. The shell model calculation of condition (2) suggests a rather pure ($\sim$94%) $\pi\{0d_{3/2}\}^{-1}\{0f_{7/2}\}^2 \otimes \nu\{0f_{7/2}\}^2$ ($\nu=5$) configuration for the $J^\pi=27/2^+$ state. The calculation also predicts closely lying two $J^\pi=25/2^+$ states, both of which have the structures of $\sim 60\% \pi\{0d_{3/2}\}^{-1}\{0f_{7/2}\}^2 \otimes \nu\{0f_{7/2}\}^2$ mixed with $\sim 30\% \pi\{0d_{3/2}\}^0\{0f_{7/2}\}^1 \otimes \nu\{d_{3/2}\}^{-1}\{0f_{7/2}\}^3$; the yrare $J^\pi=25/2_2^+$ state is predicted to lie at $\sim$1 MeV higher than the yrast $J^\pi=25/2_1^+$ state. This yrare state may be corresponding to the $J^\pi=(21/2^+,25/2^+)$ state experimentally observed at 8699 keV with a sizable intensity.

According to the calculation of condition (1), beyond the $J^\pi=15/2^+$ state which is the maximum possible angular momentum in the seniority $\nu=3$ configuration, the wave function changes its structure. The yrast states of $J^\pi=17/2^+ \sim 27/2^+$ have the predominant (>95%) $\nu=5$ structure, while the levels of $J^\pi \leqslant 15/2^+$ consist of approximately 50–60% of $\nu=5$ basis vectors and 50–40% of $\nu=3$ basis vectors. The model predicts the less regular energy spacings for the higher spin region of $J^\pi > 15/2^+$, which is also consistent with the experimental observations. As can be seen in Fig. 4, by allowing more neutrons in the $0f_{7/2}$ orbit, the energy spacings at the high-spin region become less regular and better reproduced. The seniority $\nu=1$ component shows up only in the $J^\pi=3/2^+$ state ($\sim$30%).

Thus, it may be concluded that the positive-parity bandlike structure from the $J^\pi=3/2^+$ state to the $J^\pi=(27/2^+)$ state can be described, at least qualitatively, in terms of $\{0d_{3/2},0f_{7/2},1p_{3/2}\}$ model space. The change in the energy spacings with respect to the angular momentum can be regarded as a consequence of the changes of the seniority ν of the basis vectors comprising the eigenvector of each state. It should also be noted that despite the use of the schematic interaction and the largely truncated model space, the shell model calculation could reproduce the measured electromagnetic properties fairly well.

IV. SUMMARY

In summary, the high-spin states in ^{43}Sc have been investigated by γ-γcoincidence measurement by using ^{27}Al(^{19}F,$p2n$) reaction at beam energy of 50 MeV. The $J^\pi=(17/2^-)$ state at 4382 keV and the $J^\pi=(17/2^-,21/2^-)$ state at 4633 keV were compared with the shell model calculations performed by using both the realistic two-body interaction FPD6 and the schematic interaction SDI. The $J^\pi=(17/2^-)$ state at 4382 keV is interpreted as a member of the $\{0f_{7/2}\}^3$ multiplet. Although the nature of the $J^\pi=(17/2^-,21/2^-)$ state at 4633 keV could not be determined, the lowness of the level energy indicates a sizable contribution due to the single-particle orbit(s) other than the $\{0f1p\}$. This state is clearly in need of further investigation. The positive-parity bandlike structure has been extended up to the terminating $J^\pi=(27/2^+)$ state at 8828 keV. Comparison with the shell model calculations using SDI revealed that the behavior of both energy level spacings and electromagnetic properties in this bandlike structure with respect to the increasing angular momentum can be understood in terms of the $\{0d_{3/2},0f_{7/2},1p_{3/2}\}$ shell model space and the change of seniority number (amplitude) of the eigenvectors.

ACKNOWLEDGMENTS

The authors wish to thank the crew of the JAERI tandem accelerator for providing the ^{19}F beam and for their hospitality during the experiment. We are very grateful to Emeritus Professor K. Takada of Kyushu University for his continuous and ready support in our use of the jjSMQ shell model code. The authors also express their special thanks to the National Institute of Informatics for their supporting Super SINET and to KEK Computing Research Center for HEPnet-J, which enabled efficient data transfer and timely communication among the collaborators.

[1] Z. Sawa, J. Sztarkier, and I. Bergstrom, Phys. Scr. **2**, 261 (1970).
[2] K. Nakai, B. Skaali, N. J. Sigurd Hansen, B. Herskind, and Z. Sawa, Phys. Rev. Lett. **27**, 155 (1971).
[3] J. C. Manthuruthil, C. P. Poirier, and J. Walinga, Phys. Rev. C **1**, 507 (1970).
[4] J. S. Forster, G. C. Ball, F. Ingebretsen, and C. F. Monahan, Phys. Lett. **32B**, 451 (1970).
[5] A. R. Poletti, E. K. Warburton, J. W. Olness, J. J. Kolata, and P. Gorodetzky, Phys. Rev. C **13**, 1180 (1976).
[6] L. Meyer-Schutzmeister, A. J. Elwyn, S. A. Gronemeyer, G. Hardie, R. E. Holland, and K. E. Rehm, Phys. Rev. C **18**, 1148 (1987), and references therein.
[7] E. Dafni, H. E. Mahnke, J. W. Noé, M. H. Rafailovich, and G. D. Sprouse, Phys. Rev. C **23**, 1612 (1981).
[8] I. P. Johnstone, Nucl. Phys. **A110**, 429 (1968).
[9] A. C. Merchant, J. Phys. G **10**, 885 (1984).
[10] A. C. Merchant, Phys. Rev. C **36**, 778 (1987).
[11] T. Sakuda and S. Ohkubo, Phys. Rev. C **57**, 1184 (1998).
[12] H. M. Sheppard, P. A. Butler, R. Daniel, P. J. Nolan, N. R. F.

Ramano, and J. F. Sharphey-Scharfer, J. Phys. G **6**, 511 (1980).
[13] K. Furuno *et al.*, Nucl. Instrum. Methods Phys. Res. A **421**, 211 (1999).
[14] J. F. Ziegler, http://www.srim.org
[15] M. Piiparinen *et al.*, Nucl. Phys. **A605**, 191 (1996).
[16] J. A. Cameron and B. Singh, Nucl. Data Sheets **92**, 783 (2001).
[17] *Table of Isotopes CD-ROM*, 8th ed., edited by R. B. Firestone (Wiley-Interscience, New York, 1999), 1999 Update.
[18] K. Takada, M. Sato, and S. Yasumoto, (private communication). Source codes and binaries are available at ftp://ftp.kutl.kyushu-u.ac.jp/pub/takada/jjSMQ/
[19] W. A. Richter, M. G. V. D. Merwe, R. E. Julies, and B. A. Brown, Nucl. Phys. **A523**, 325 (1991).
[20] R. Arivieu and S. A. Moszkowski, Phys. Rev. **145**, 830 (1966).
[21] A. Plastino, R. Arivieu, and S. A. Moszkowski, Phys. Rev. **145**, 837 (1966).
[22] P. W. M. Glaudemans, P. J. Brussaard, and B. H. Wildenthal, Nucl. Phys. **A102**, 593 (1967).
[23] P. W. M. Glaudemans, M. J. A. D. Voigt, and E. F. M. Steffence, Nucl. Phys. **A198**, 609 (1972).
[24] P. J. Brussaard and P. W. M. Glaudemans, *Shell-Model Applications in Nuclear Spectroscopy* (North-Holland, Amsterdam, 1977), Chap. 6.
[25] M. J. Taylor *et al.*, Phys. Lett. B **559**, 187 (2003).
[26] S. Schielke *et al.*, Phys. Lett. B **571**, 29 (2003).
[27] C. K. Davis, G. D. Jones, I. G. Main, B. T. McCrone, M. F. Thomas, and P. J. Twin, J. Phys. A **6**, 844 (1973).